

A non-resonant dark-side solution to the solar neutrino problem

O. G. Miranda², C. Peña-Garay¹, T. I. Rashba³, V. B. Semikoz³
and J. W. F. Valle¹

¹*Instituto de Física Corpuscular – C.S.I.C., Universitat de València
Edificio Institutos, Apt. 22085, E-46071 València, Spain*

²*Departamento de Física, Centro de Investigación y de Estudios Avanzados Apdo.
Postal 14-740 07000 Mexico, DF, Mexico*

³*Institute of Terrestrial Magnetism, Ionosphere and Radio Wave Propagation of
the Russian Academy of Sciences, 142190, Troitsk, Moscow region, Russia*

Abstract

We re-analyse spin-flavour precession solutions to the solar neutrino problem in the light of the recent SNO CC result as well as the 1258-day Super-Kamiokande data and the upper limit on solar anti-neutrinos. In a self-consistent magneto-hydrodynamics approach the resulting scheme has only 3 effective parameters: Δm^2 , μB_\perp and the neutrino mixing angle θ . We show how a rates-only analysis for fixed μB_\perp slightly favours spin-flavour precession (SFP) solutions over oscillations (OSC). In addition to the resonant solution (RSFP for short), there is a new non-resonant solution (NRSFP) in the “dark-side”. Both RSFP and NRSFP lead to flat recoil energy spectra in excellent agreement with the latest SuperKamiokande data. We also show that in the presence of a neutrino transition magnetic moment of 10^{-11} Bohr magneton, a magnetic field of 80 KGauss eliminates all large mixing solutions other than the so-called LMA solution.

Key words: neutrino oscillations, solar neutrinos, neutrino mass and mixing, neutrino magnetic moment

PACS: 14.60.Pq, 26.65.+t, 13.15.+g

Email addresses: Omar.Miranda@fis.cinvestav.mx (O. G. Miranda²),
penya@hal.ific.uv.es (C. Peña-Garay¹), rashba@izmiran.rssi.ru (T. I.
Rashba³), semikoz@orc.ru, semikoz@ific.uv.es (V. B. Semikoz³),
valle@ific.uv.es (J. W. F. Valle¹).

1 Introduction

The recent charged current measurement at the Sudbury Neutrino Observatory (SNO) [1] has shed more light on the long-standing problem posed by the previous solar neutrino data [2] forcing us to reconsider the status of the various solutions to the solar neutrino anomaly.

In this paper we re-consider the case of spin-flavour precession solutions, based on non-zero transition magnetic moments of neutrinos [3]. These are especially attractive for several reasons: (i) on general theoretical grounds [4] neutrinos are expected to be Majorana particles; (ii) such conversions induced by transition magnetic moments may be resonantly amplified in the Sun [5]; (iii) they offer the best pre-SNO global fit of solar neutrino data [6], and (iv) an SFP type solution, being an active-to-active conversion mechanism, has the right features to reconcile the SNO CC and SuperKamiokande results.

Finally, such solutions are rather robust if the arbitrariness in the choice of the magnetic field profile in the solar convective zone [7–9] is removed in a self-consistent way from magneto-hydrodynamics theory [6].

By generalizing our previous work [6] to the case of non-zero neutrino mixing we obtain two new and important results: (i) we recover the resonant small-mixing solution to the solar neutrino problem found previously [6] and analyse its status in the light of the new SNO and 1258-day SK results, and (ii) we find a genuinely new non-resonant SFP solution in the so-called dark-side of the neutrino mixing parameter [10,11]. Following [12] we choose to determine the allowed solutions by considering only the total rates of the solar neutrino experiments, ignoring first all the data from the Super-Kamiokande measurements of the spectral energy distribution and the day-night variations. We find that these solutions, both the resonant spin flavour precession solution (which we call RSFP) as well as a new non-resonant one (NRSFP solution), provide excellent descriptions of the solar rates, including the recent SNO CC result. Subsequently we demonstrate how these solutions predict a substantially flat recoil energy spectrum of solar neutrinos in agreement with the observations of the Super-Kamiokande experiment [2]. Moreover, our solutions are consistent with the non-observation of electron anti-neutrinos from the sun [13,14] in the results of the LSD experiment [15] as well as SuperKamiokande [16].

This paper is organized as follows. In section 2 we discuss the neutrino evolution and conversion probabilities, in section 3 we summarize the calculational and fit procedures we adopt, while we summarize our results in section 4.

2 Neutrino Evolution and Survival/Conversion Probabilities

Motivated by the results from reactor neutrino experiments [17] and to some extent also from atmospheric neutrinos [18] we adopt, for simplicity, a two-flavour RSFP scenario. The Majorana neutrino evolution Hamiltonian in a magnetic field in this case is well-known to be four-dimensional [3],

$$i \begin{pmatrix} \dot{\nu}_{eL} \\ \dot{\bar{\nu}}_{eR} \\ \dot{\nu}_{\mu L} \\ \dot{\bar{\nu}}_{\mu R} \end{pmatrix} = \begin{pmatrix} V_e - c_2\delta & 0 & s_2\delta & \mu B_+(t) \\ 0 & -V_e - c_2\delta & -\mu B_-(t) & s_2\delta \\ s_2\delta & -\mu B_+(t) & V_\mu + c_2\delta & 0 \\ \mu B_-(t) & s_2\delta & 0 & -V_\mu + c_2\delta \end{pmatrix} \begin{pmatrix} \nu_{eL} \\ \bar{\nu}_{eR} \\ \nu_{\mu L} \\ \bar{\nu}_{\mu R} \end{pmatrix}, \quad (1)$$

where $c_2 = \cos 2\theta$, $s_2 = \sin 2\theta$, $\delta = \Delta m^2/4E$, assumed to be always positive, are the neutrino oscillation parameters; μ is the neutrino transition magnetic moment; $B_\pm = B_x \pm iB_y$, are the magnetic field components which are perpendicular to the neutrino trajectory; $V_e(t) = G_F\sqrt{2}(N_e(t) - N_n(t)/2)$ and $V_\mu(t) = G_F\sqrt{2}(-N_n(t)/2)$ are the neutrino vector potentials for ν_{eL} and $\nu_{\mu L}$ in the Sun, given by the number densities of the electrons ($N_e(t)$) and neutrons ($N_n(t)$). When $\theta \rightarrow 0$ we recover the case treated in [6] while as $B \rightarrow 0$ we recover the pure OSC case. In our calculations of P_i we use the electron and neutron number densities from the BP00 model [19] with the magnetic field profile obtained in ref. [6] for $k=6$ and $R_0 = 0.6R_\odot$. We assume a transition magnetic moment of 10^{-11} Bohr magneton, consistent with experiment and a magnetic field magnitude around 80 kGauss, allowed by helioseismological observations. Finally, in order to obtain Earth matter effects we integrate numerically the evolution equation in the Earth matter using the Earth density profile given in the Preliminary Reference Earth Model (PREM) [20].

2.1 The solar neutrino conversion probability

The combined amplitude for a solar ν_e to be detected as ν_α (α being e , μ , \bar{e} , $\bar{\mu}$) with energy E at a detector in the Earth can be written as:

$$A_{\nu_e \rightarrow \nu_\alpha}^{\text{S-V-E}} = \langle \nu_\alpha | U^{\text{Earth}} U^{\text{Vacuum}} U^{\text{Sun}} | \nu_e \rangle = \sum_{i=1,2,\bar{1},\bar{2}} A_{ei}^S A_{i\alpha}^E \exp[-im_i^2(L - R_\odot)/2E]. \quad (2)$$

Here A_{ei}^S is the amplitude of the transition $\nu_e \rightarrow \nu_i$ (ν_i is the i -mass eigenstate) from the production point to the Sun surface, $A_{i\alpha}^E$ is the amplitude of the transition $\nu_i \rightarrow \nu_\alpha$ from the Earth surface to the detector, and the propagation

in vacuum from the Sun to the surface of the Earth is given by the exponential, where L is the distance between the center of the Sun and the surface of the Earth, and R_\odot is the radius of the Sun. While the presence of magnetic field couples the four states in the evolution, its absence in vacuum and in the Earth produces the decoupling of the four states into two doublets : (ν_e, ν_μ) and ($\nu_{\bar{e}}, \nu_{\bar{\mu}}$). The corresponding probabilities $P_{e\alpha}$ are then given by:

$$P_{ee} = P_1 P_{1e} + P_2 P_{2e} + 2\sqrt{P_1 P_2 P_{1e} P_{2e}} \cos \xi_1 \quad (3)$$

$$P_{e\mu} = P_1 P_{1\mu} + P_2 P_{2\mu} - 2\sqrt{P_1 P_2 P_{1\mu} P_{2\mu}} \cos \xi_1 \quad (4)$$

$$P_{e\bar{e}} = P_1 P_{1\bar{e}} + P_2 P_{2\bar{e}} - 2\sqrt{P_1 P_2 P_{1\bar{e}} P_{2\bar{e}}} \cos \xi_2, \quad (5)$$

$$P_{e\bar{\mu}} = P_1 P_{1\bar{\mu}} + P_2 P_{2\bar{\mu}} + 2\sqrt{P_1 P_2 P_{1\bar{\mu}} P_{2\bar{\mu}}} \cos \xi_2. \quad (6)$$

Here $P_i \equiv |A_{ei}^S|^2$ is the probability that the solar neutrinos reach the surface of the Sun as $|\nu_i\rangle$, while $P_{i\alpha} \equiv |A_{i\alpha}^E|^2$ is the probability of ν_i arriving at the surface of the Earth to be detected as ν_α . The phases ξ_a ($a = 1, 2$) are given by

$$\xi_a = \frac{\Delta m^2 (L - R_\odot)}{2E} + \phi_a, \quad (7)$$

where ϕ_a contain the phases due to propagation in the Sun and in the Earth and we checked that it can be safely neglected for our purposes.

The results presented in the following sections have been obtained using the general expression for the probabilities with $P_1, P_2, P_{\bar{1}}$ and P_{2e} found by numerically solving the evolution equation (1). The probabilities required in Eq. (4) are not independent from the last ones and can be obtained using the unitarity relations and using relations between both octants in mixing for the evolution in the Earth, ie., $P_{1\bar{e}}(\theta) = P_{2e}(\frac{\pi}{2} - \theta)$. In the limit $B_\perp \rightarrow 0$ we recover the forms given in ref. [21]. In Fig. 1 we show a schematic view of the spin flavour precession survival probabilities both in the “light” and “dark” sides. The first corresponds to $0 \leq \theta \leq \pi/4$ while the latter means $\pi/4 \leq \theta \leq \pi/2$. The dotted curve corresponds to the RSFP case, while the solid one will lead to the new non-resonant NRSFP solution, see below. One notices that, in contrast to the oscillation case, the asymptotic value of the survival probability in the SFP model can be lower than 0.5 as $E \rightarrow \infty$ or $\Delta m \rightarrow 0$. This can be understood as follows. Consider the idealized case of constant matter potential, constant magnetic field over a finite slab Δr and $\cos 2\theta \approx \pm 1$. In this case one can write simple analytic formulae for the neutrino conversion probabilities. For

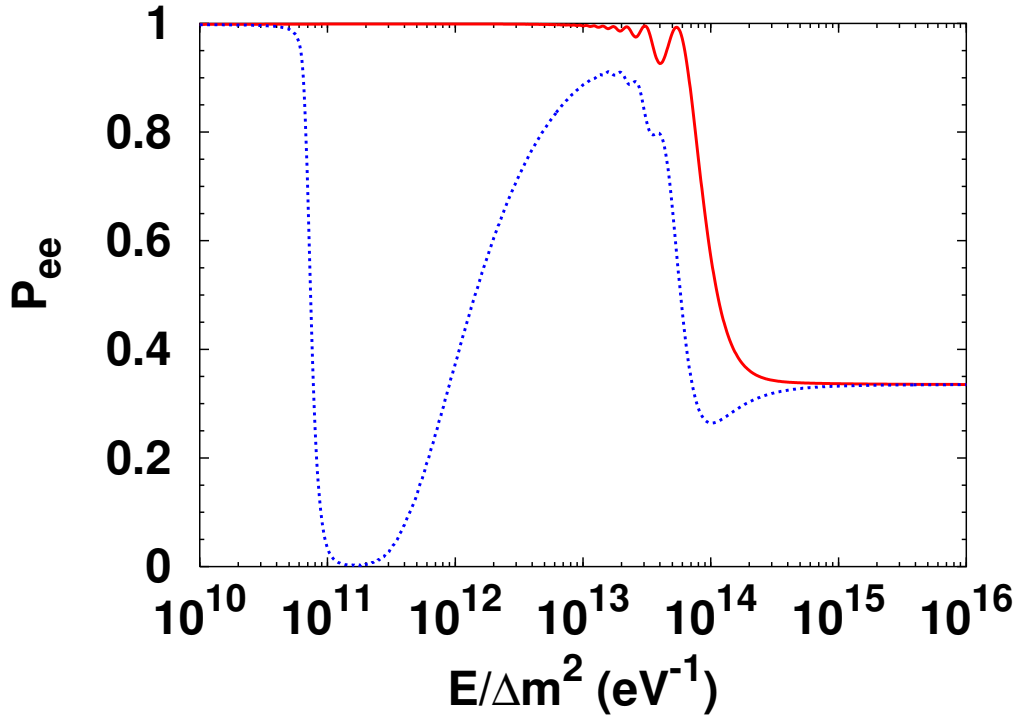


Fig. 1. Neutrino spin flavour precession survival probabilities in “light” and “dark” sides, for $\mu = 10^{-11} \mu_B$ and $B_{\perp} \sim 80$ kGauss.

example the ν_e survival probability may be given as

$$P_{ee} = 1 - \frac{(2\mu_{\nu}B_{\perp})^2}{(V_e + V_{\mu} - 2\delta \cos 2\theta)^2 + (2\mu_{\nu}B_{\perp})^2} \times \sin^2 \left(\sqrt{(V_e + V_{\mu} - 2\delta \cos 2\theta)^2 + (2\mu_{\nu}B_{\perp})^2} \frac{\Delta r}{2} \right) . \quad (8)$$

For the case $\cos 2\theta \approx 1$ we obtain the well-known resonant solution, while the alternative $\cos 2\theta \approx -1$ choice corresponds to our new NRSFP solution in the dark side, see below. The higher asymptotic suppression of P_{ee} in both cases implies a higher possible degree of suppression of ^8B neutrinos than achievable in the OSC case. Moreover the converted $\bar{\nu}_{\mu}$ can be detected via the neutral current, thus reconciling the SNO CC result with the higher Super-Kamiokande rate measurement.

3 Calculational Method

In our following description of solar neutrino data [2] we adopt the analysis techniques which have already been presented in previous papers [12,18,22] using the theoretical BP00 standard solar model best-fit fluxes and estimated uncertainties from ref. [19]. In addition to the solar data [2] we also use the

reactor data [17] as well as the data on searches for anti-neutrinos from the sun [15]. For the neutrino conversion probabilities we use the numerical results calculated in the previous section.

We employ the self-consistent magneto-hydrodynamics magnetic field profile obtained in ref. [6] for $k=6$ and $R_0 = 0.6R_\odot$. The resulting theoretical framework has therefore only 2 effective free parameters: Δm^2 , $\tan^2 \theta$. The remaining parameter μB_\perp characterizing the maximum magnitude of the magnetic field in the convective zone has been fixed at its optimum value. Since the parameter space is three-dimensional, the allowed regions for a given C.L. are defined as the set of points satisfying the condition

$$\chi_{\text{SOL}}^2(\Delta m^2, \theta, \mu B_\perp) - \chi_{\text{SOL},\text{min}}^2 \leq \Delta\chi^2(\text{C.L.}, 2 \text{ d.o.f.}), \quad (9)$$

where χ_{SOL}^2 contains

$$\chi_{\text{LSD}}^2(\Delta m^2, \theta, \mu B_\perp) = \frac{\left(N_{\bar{\nu}_e}^{\text{TH}}(\Delta m^2, \theta, \mu B_\perp) - N_{\bar{\nu}_e}^{\text{EXP}}\right)^2}{\sigma_{\text{LSD}}^2} \quad (10)$$

where $N_{\bar{\nu}_e}^{\text{EXP}} = -1.5$ and $\sigma_{\text{LSD}} = 22$ in order to account for the data on searches for anti-neutrinos from the sun [15]. As we will see this term plays an important role in restricting the neutrino parameters.

In our numerical calculations we use the survival/conversion probabilities of solar electron neutrino valid in the full range of Δm^2 and θ , selecting the optimum value of μB_\perp with B_\perp varying over the range from 0 to 100 kGauss ¹.

Finally, we employ the relevant reaction cross sections and efficiencies for the all experiments used in ref. [12,18,22]. For the SNO case the CC cross section for deuterium was taken from [24].

3.1 Rate Fit

Here we take into account the total rates in the chlorine, gallium, and Super-Kamiokande experiments, the SNO CC result and the anti-neutrino limit from LSD, and also the reactor neutrino data [17]. The rates from the GALLEX/GNO experiments have been averaged so as to provide a unique data point. The resulting number of degrees of freedom is therefore 4: 4 (rates) + SNO + LSD - 2 (parameters: Δm^2 , θ) with a fixed μB_\perp .

We present in Fig. 2 the allowed solutions for the two-flavour SFP case. These include the pure two-neutrino oscillation case, as well as the conventional RSFP and the new NRSFP solution.

¹ A description of this procedure will be presented elsewhere [23].

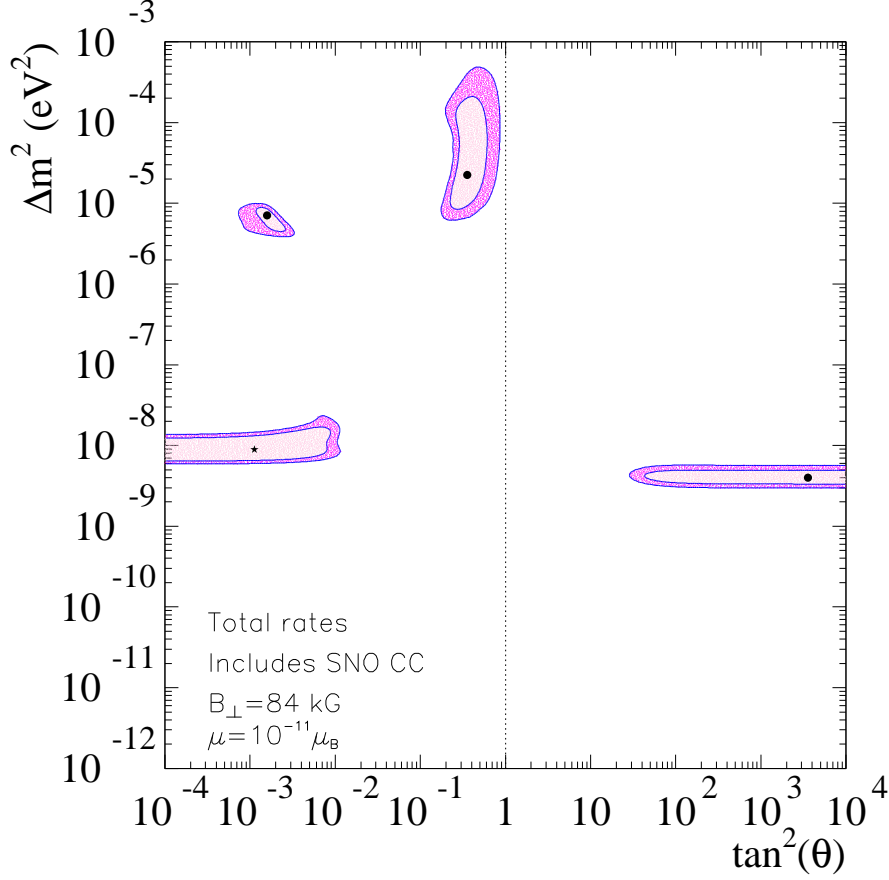


Fig. 2. Allowed solutions to the solar neutrino rates and reactor data for $\mu_\nu = 10^{-11}\mu_B$ and $B_\perp = 84$ kGauss. The upper limit on the solar anti-neutrino flux according to LSD data is included.

Note that the contours refer to 90%, 99% CL defined with respect to the global minimum of χ^2 . We find that both LMA and SMA oscillation solutions are recovered without an essential change due to the effect of the magnetic moment. The SMA solution appears (even though disfavored), but leads to an unacceptably tilted recoil energy spectrum, as will be seen in Fig. 3.

An important point to notice is that this plot lacks the LOW solution as well as the characteristic region joining it through the dark side to the vacuum-type solutions [23]. In this figure we have adjusted the value of μB_\perp to its best value (for $\mu = 10^{-11}$ Bohr magneton this corresponds to $B_\perp \sim 80$ kGauss). One sees that the relatively large μ value has important consequences. It leads in this case in the complete absence of all large mixing solutions other than the LMA solution due to the effect magnetic field. Such a value implies an important modification in the neutrino survival probability implying an unwanted over-suppression of the ^8B neutrino flux and therefore the impossibility to account for all experiments in this region because of the high $\bar{\nu}_e$ flux. From this point of view vacuum-type solutions are *unstable* against the effect of the magnetic

field. In fact the non-LMA large mixing OSC solutions are not re-instated even if the ^8B neutrino flux is left free. The goodness of fit of the various solutions in Fig. 2 is given in table 1. One notices that, of the OSC-type solutions, LMA is the best ². However the SFP solutions are slightly better.

Solution	Δm^2	$\tan^2(\theta)$	χ^2_{\min}	g.o.f.
LMA	2.1×10^{-5}	0.34	3.99	14%
SMA	6.9×10^{-6}	1.6×10^{-3}	5.25	7%
RSF	8.9×10^{-9}	1.1×10^{-3}	2.98	22%
NRSF	4.0×10^{-9}	3.5×10^3	3.83	15%

Table 1

Best-fit points and goodness-of-fit of oscillation and spin flavour solutions to the solar neutrino problem as determined from the rates-only analysis for $\mu = 10^{-11} \mu_B$ and $B_{\perp} = 84$ kGauss.

Note that the goodness-of-fit given in the last column is calculated using the value of $\chi^2/\text{d.o.f}$ for each allowed solution corresponding to each of the local minima of table 1. Note also that should we perform a restricted two-parameter analysis using only Δm^2 and the neutrino mixing angle θ for the pure OSC case and only Δm^2 and μB_{\perp} for the pure SFP case we obtain exactly the same goodness-of-fit and χ^2_{MIN} for each of the corresponding SFP and OSC solutions in table 1.

A more striking feature of Fig. 2 is the appearance of two new solutions which are totally due to the effect of the magnetic field. One contains the previous resonant no-mixing solution which is recovered, after updating the solar data to the measurements from 1258 days of Super-Kamiokande data and SNO CC measurement. One sees that this RSFP solution extends up to $\tan^2 \theta$ values around 10^{-2} or so. More importantly, one finds a genuinely new non-resonant (NRSFP) solution in the “dark-side” of the parameter space, for large $\tan^2 \theta$ values. The existence of these solutions can be easily understood on the basis of Fig. 1. Similarly one can understand the non-resonant nature of the new NRSFP solution. Note that in obtaining the shape of the RSF solutions we have made use of the data on searches for anti-neutrinos from the sun [15]. These play an important role in cutting the non-resonant RSF solution to $\tan^2 \theta$ values larger than about 30.

² The first time the LMA solution was shown to be the best OSC solution was in [22] due to the details of the solar neutrino spectra measured at Super-Kamiokande. This trend is now re-inforced by the enhanced statistics. The SNO CC rate-result implies, on its own, a preference for the LMA if the BP00 boron flux is assumed

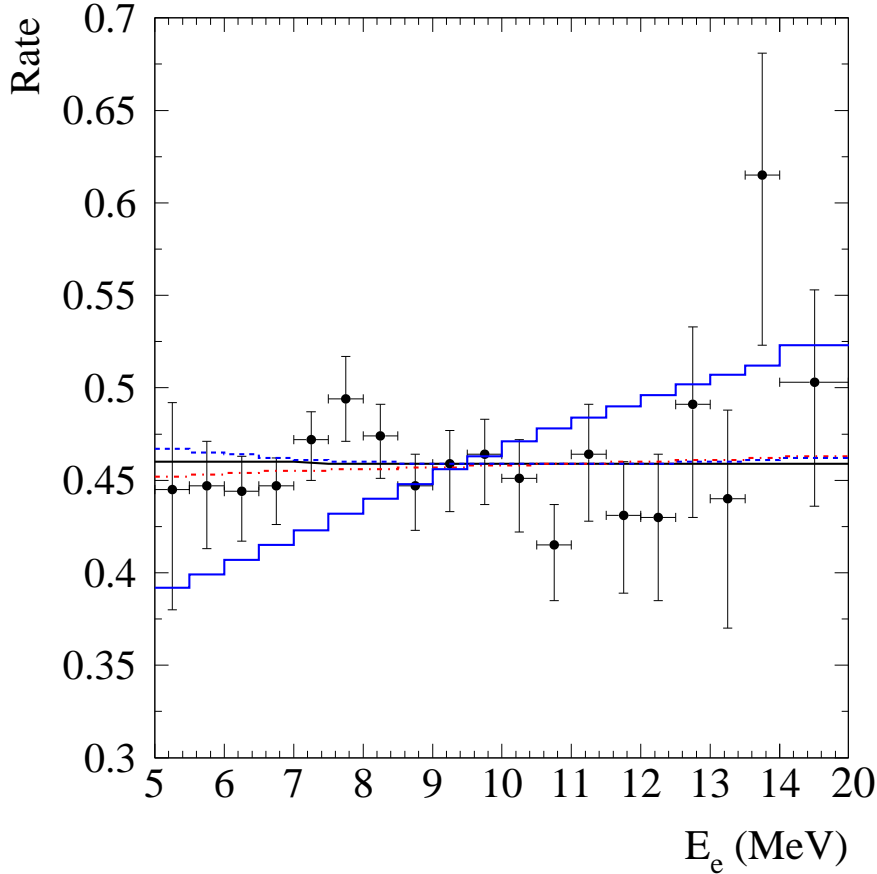


Fig. 3. Predicted recoil energy spectra for spin flavour precession solutions. Details in text.

3.2 Recoil Spectra

We now present the predicted day–night averaged ³ spectral energy distribution for our two spin flavour precession solutions and compare it with those of the pure OSC-type solutions.

In Fig. 3 we present the recoil energy spectra for spin flavour precession. The thin solid horizontal line corresponds to the new NRSFP solution, while the dot-dashed refers to the standard RSFP solution. Clearly both spin flavour precession spectra are totally consistent with the Super-Kamiokande data and, as a result, will remain as excellent solutions after the inclusion of the recoil energy spectra. We also present the predicted oscillation spectra, in solid that of the SMA solution and dashed the LMA solution. Clearly one can see that, in contrast with the RSFP and NRSFP solutions, the SMA spectrum is in strong disagreement with the SK data. A full-fledged global fit of the recoil

³ Note that, in contrast to the OSC spectra, where a day–night effect is predicted, the SFP spectra show no day–night asymmetry.

spectra for the spin flavour solutions is outside the scope of this letter and will be presented elsewhere [23].

4 Summary and Discussion

In this paper we have re-considered the case of spin-flavour precession solutions, based on non-zero transition magnetic moments of Majorana neutrinos taking into account the recent SNO CC result as well as the 1258-day solar neutrino data from Super-Kamiokande. We have also paid attention to the upper limit on the solar anti-neutrino flux from the LSD experiment as well as the reactor neutrino data. We have followed the self-consistent approach from magneto-hydrodynamics theory employed previously [6] in order to remove the arbitrariness associated to the magnetic field profile [7–9]. This effectively reduces the theoretical analysis framework to a three-parameter one. In-so-doing we have also generalized our previous work [6] to the case of non-zero neutrino mixing, performing the first “unified” study of solar neutrino data in the presence of a neutrino transition magnetic moment. It contains as particular cases “light-side” and “dark-side” OSC as well as genuine SFP solutions.

We have recovered the standard resonant small-mixing solution to the solar neutrino problem (RSFP) which remains as best solution to the solar neutrino anomaly (see table). Second, we have found a genuinely new non-resonant solution in the so-called “dark-side” of the neutrino mixing parameter. Such NRSFP solution gives a very good fit of the present solar neutrino data. Although we have chosen to determine the allowed solutions by considering only the total rates of the solar neutrino experiments, we have presented their predicted recoil spectra, showing how they are in agreement with the data from the Super-Kamiokande experiment. A full comparative study of oscillation and spin flavour solutions of the solar neutrino problem is outside the scope of this letter and will be presented elsewhere [23].

Acknowledgements

We would like to thank Alexei Bykov, Hiroshi Nunokawa, Alexander Rez, Victor Popov and Dmitri Sokoloff for very useful discussions. This work was supported by Spanish grants PB98-0693 and GV99-3-1-01, by the European Commission RTN network HPRN-CT-2000-00148 and by the European Science Foundation network grant N. 86. VBS and TIR were partially supported by the RFBR grants 00-02-16271 and 01-02-06225 and OGM was supported by the CONACyT-Mexico grants J32220-E and 35792-E. TIR and OGM thank

the València Astroparticle and High Energy Physics Group for the kind hospitality.

References

- [1] Q. R. Ahmad *et al.* [SNO Collaboration], nucl-ex/0106015.
- [2] B.T. Cleveland *et al.*, *Astrophys. J.* **496** (1998) 505; K.S. Hirata *et al.*, Kamiokande Coll., *Phys. Rev. Lett.* **77** (1996) 1683; W. Hampel *et al.*, GALLEX Coll., *Phys. Lett. B* **447** (1999) 127; D.N. Abdurashitov *et al.*, SAGE Coll., *Phys. Rev. Lett.* **83** (1999) 4686; *Phys. Rev. C* **60** (1999) 055801 [astro-ph/9907113]; V. Gavrin (SAGE Collaboration), *Nucl. Phys. Proc. Suppl.* **B 91** (2001) 36; M. Altmann *et al.* (GNO Collaboration), *Phys. Lett. B* **490** (2000) 16; E. Bellotti *et al.* (GNO Collaboration), *Nucl. Phys. Proc. Suppl.* **B 91** (2001) 44; Y. Fukuda *et al.* (Super-Kamiokande Collaboration), *Phys. Rev. Lett.* **81** (1998) 1158; Erratum **81** (1998) 4279; *Phys. Rev. Lett.* **82** (1999) 1810; Y. Suzuki (Super-Kamiokande Collaboration), *Nucl. Phys. Proc. Suppl.* **B 91** (2001) 29; S. Fukuda *et al.* (Super-Kamiokande Collaboration), *Phys. Rev. Lett.* **86** (2001) 5651.
- [3] J. Schechter and J. W. F. Valle, *Phys. Rev.* **D24** (1981) 1883; Erratum-ibid. **D25** (1982) 283
- [4] J. Schechter and J. W. F. Valle, *Phys. Rev.* **D22** (1980) 2227.
- [5] E. K. Akhmedov, *Phys. Lett. B* **213** (1988) 64; C. Lim and W. J. Marciano, *Phys. Rev. D* **37** (1988) 1368.
- [6] O. G. Miranda, C. Pena-Garay, T. I. Rashba, V. B. Semikoz and J. W. F. Valle, *Nucl. Phys. B* **595** (2001) 360 [hep-ph/0005259].
- [7] E. K. Akhmedov and J. Pulido, *Phys. Lett. B* **485** (2000) 178 [hep-ph/0005173]; *Astropart. Phys.* **13** (2000) 227 [hep-ph/9907399].
- [8] M. M. Guzzo and H. Nunokawa, *Astropart. Phys.* **12** (1999) 87 [hep-ph/9810408]. H. Nunokawa and H. Minakata, *Phys. Lett. B* **314** (1993) 371.
- [9] J. Derkaoui and Y. Tayalati, *Astropart. Phys.* **14** (2001) 351 [hep-ph/9909512].
- [10] G. L. Fogli, E. Lisi and D. Montanino, *Phys. Rev. D* **54** (1996) 2048 [hep-ph/9605273].
- [11] A. de Gouvea, A. Friedland and H. Murayama, *Phys. Lett. B* **490** (2000) 125 [hep-ph/0002064].
- [12] J. N. Bahcall, M. C. Gonzalez-Garcia and C. Pena-Garay, hep-ph/0106258. For recent papers on the oscillation interpretation of the solar neutrino anomaly after the SNO result see [25].

- [13] R. Barbieri, G. Fiorentini, G. Mezzorani and M. Moretti, Phys. Lett. B **259** (1991) 119.
- [14] P. Vogel and J. F. Beacom, Phys. Rev. D **60** (1999) 053003 [hep-ph/9903554].
- [15] M. Aglietta *et al.*, JETP Lett. **63** (1996) 791 [Pisma Zh. Eksp. Teor. Fiz. **63** (1996) 753].
- [16] M.B. Smy, private communication; C. Yanagisawa, Talk given at the Euroconference on Frontiers on Cosmology and Astroparticle Physics, Saint Feliu de Guixols, Spain, Proceedings Supplements, 2001, Vol. 95, ISSN 0920-5632
- [17] M. Apollonio *et al.* [CHOOZ Collaboration], Phys. Lett. B **466**, 415 (1999) [hep-ex/9907037].
- [18] See, for example, M. C. Gonzalez-Garcia, M. Maltoni, C. Pena-Garay and J. W. F. Valle, Phys. Rev. D **63** (2001) 033005 [hep-ph/0009350], G. L. Fogli in *Neutrino Telescopes 2001*, Venice, Italy, March 2001
- [19] <http://www.sns.ias.edu/~jnb/SNdata/Export/BP2000>; J. N. Bahcall, S. Basu and M. H. Pinsonneault, Astrophys. J. **529**, 1084 (2000); Astrophys. J. **555** (2001) 990
- [20] A. M. Dziewonski and D. L. Anderson, Phys. Earth Planet. Inter. **25**, 297 (1981).
- [21] M. C. Gonzalez-Garcia and C. Pena-Garay, Nucl. Phys. Proc. Suppl. **91** (2000) 80 [hep-ph/0009041]. For a 3-parameter study using this method see ref. [18].
- [22] M. C. Gonzalez-Garcia, P. C. de Holanda, C. Pena-Garay and J. W. F. Valle, Nucl. Phys. **B573** (2000) 3 [hep-ph/9906469] and references therein.
- [23] For a complete discussion see O. Miranda *et al.*, in preparation.
- [24] J.F. Beacom and S.J. Parke, [hep-ph/0106128]; S. Nakamura, T. Sato, V. Gudkov and K. Kubodera, Phys. Rev. C **63** (2001) 034617; M. Butler, J.-W. Chen and X. Kong, Phys. Rev. C **63** (2001) 03550; I.S. Towner, Phys. Rev. C **58** (1998) 1288.
- [25] A. Bandyopadhyay, S. Choubey, S. Goswami and K. Kar, hep-ph/0106264. G. L. Fogli, E. Lisi, D. Montanino and A. Palazzo, hep-ph/0106247. P. Creminelli, G. Signorelli and A. Strumia, hep-ph/0102234 (version 2); V. Barger, D. Marfatia and K. Whisnant, hep-ph/0106207.